

Single-cluster-update Monte Carlo method for the random anisotropy model

U. K. Rößler

Institut für Festkörper- und Werkstofforschung Dresden e.V., Postfach 270016, D-01171 Dresden, Germany

(Received 19 January 1999)

A Wolff-type cluster Monte Carlo algorithm for random magnetic models is presented. The algorithm is demonstrated to reduce significantly the critical slowing down for planar random anisotropy models with weak anisotropy strength. Dynamic exponents $z \lesssim 1.0$ of best cluster algorithms are estimated for models with ratio of anisotropy to exchange constant $D/J = 1.0$ on cubic lattices in three dimensions. For these models, critical exponents are derived from a finite-size scaling analysis. [S0163-1829(99)03818-7]

There is ongoing interest in the properties of random magnets¹ and related systems like disordered type-II superconductors,² superfluids, or density waves pinned in rough media.^{3,4} In particular, models with continuous spins (Heisenberg or XY model) were studied recently⁵ because the stability of ferromagnetic or quasi-long-range order subject to weak quenched disorder is not completely understood. For two-component spins the transition might resemble that of the corresponding pure system, which is the Kosterlitz-Thouless transition of the pure XY model in $d=2$ dimensions,⁶ and the XY-ferromagnetic transition in $d=3$. On the other hand, such systems may eventually undergo a transition to a spin-glass phase.⁷⁻¹⁰ Thus the critical properties of such disordered magnetic systems are not well understood, and related numerical studies are desirable.

Monte Carlo (MC) simulation methods provide powerful tools to investigate statistical models. However, MC simulation using single spin-flip dynamics, e.g., the Metropolis algorithm, is plagued by critical slowing down because of diverging correlation lengths and times.¹¹ Cluster MC dynamics devised by Swendsen and Wang (SW) can reduce slowing down drastically for some (mostly unfrustrated) systems.¹² By deleting and freezing bonds, SW algorithms decompose the systems into independent clusters of many spins which can be flipped coherently by collective updates. Wolff developed an even more efficient single-cluster-update algorithm,¹³ where only one cluster is grown in each step. Wolff's method proved to reduce slowing down by orders of magnitudes for pure $d=2,3$ XY models allowing progress with numerical studies of their properties.¹⁴ Generally, new types of cluster algorithms for special classes of models are important tools for a better understanding of their properties, because these are related to the percolative properties of the clusters.¹⁵

Here, we extend Wolff's cluster algorithm to models of magnetic systems with random potential terms. Examples of such systems are random anisotropy¹⁶ (RAM) or random-field models.¹⁷ The physics of these models is concerned with pinning which entails frustrations between the bonds in the spins system and its deformations in the random potential. So, any cluster method for this type of model has to incorporate pinning of the clusters.

Our approach is similar in spirit to the usage of *ghost spins* with SW or Wolff algorithms^{12,18} for spin models in an external field. Thus the on-site random potentials are viewed

as additional bonds to some spin entity outside of the system, which does not take part in the MC dynamics. In SW-type cluster methods, pinning occurs if such a bond at a site or a group of sites in a growing cluster is frozen. So far, such an extension was proposed only in an *ad hoc* fashion by Dotenko, Selke, and Talapov (DST).¹⁹ In the DST approach a cluster is grown first by deleting and freezing bonds as in the Wolff algorithm and then the sum of all on-site potentials for this cluster is considered as one bond to a single *ghost spin*. Sampling this term determines whether the cluster is pinned or can be flipped. This method is inefficient because clusters grow too large and most of them have to be rejected when the pinning potential is finally considered. Barkema and Marko²⁰ improved and implemented the method with their limited-cluster-flip (LCF) algorithm for random-field Ising models by imposing further constraints which stop cluster growth at some stage. Our central idea is that sampling the on-site potential terms can be efficiently done during cluster growth. Cluster growth is stopped by the random potential itself as soon as a pinning site or group of sites is found. Thus this method probes the real limitations on shapes and sizes of clusters in the system. Artificial constraints as in the LCF approach are not necessary, but they can be superimposed if desired.

Our algorithm will be described and demonstrated for random anisotropy XY models, but an adaption to other similar random systems is possible. To be specific, we use random anisotropy models, proposed by Harris, Plischke, and Zuckermann,¹⁶ considered as classical spin system:

$$H = -J \sum_{\langle i,j \rangle} \mathbf{S}_i \cdot \mathbf{S}_j - D \sum_{i=1}^N (\mathbf{S}_i \cdot \mathbf{a}_i)^2 \quad (J > 0). \quad (1)$$

In Eq. (1) the spins \mathbf{S}_i and the random axes \mathbf{a}_i are unit vectors with m components. The \mathbf{a}_i are uncorrelated with isotropic distribution, defining the quenched disorder. For tests of our algorithm, we consider this system with $m=2$ in $d=2$ (3) dimensions on square (cubic) lattices with $N \equiv L^d$ sites, using periodic boundary conditions.

The simplest form of the algorithm generates clusters as follows: (a) To start growth, choose a random plane for reflections of the spins, as in the original Wolff algorithm, and a random site as starting point, mark it, and put it first on a list which enumerates the sites belonging to the growing cluster. (b) Growth from the starting site is done iteratively:

Any listed site in the cluster is visited once in order to sample its on-site potential energy and its bonds to spins outside the growing cluster. So, take an entry i from this list, which was not visited yet, and calculate for spin i the changed spin direction \mathbf{S}_i' and the associated change of the on-site potential energy: $\Delta E_i^a = -D[(\mathbf{S}_i' \cdot \mathbf{a}_i)^2 - (\mathbf{S}_i \cdot \mathbf{a}_i)^2]$. (c) Decide whether the on-site potential at site i does not pin the cluster with a thermal probability

$$P_i^a(\mathbf{S}_i'; \mathbf{S}_i) = \exp(\min\{0, -\beta \Delta E_i^a\}), \quad (2)$$

where β is the inverse temperature $1/T$. If the cluster is pinned its move must be rejected. Then start again with step (a). (d) Otherwise, visit all nearest neighbors j of site i . If j is not yet on the list of spins in the cluster determine whether the bond between i and j is frozen with a probability:

$$P^b(\mathbf{S}_i'; \mathbf{S}_i, \mathbf{S}_j) = 1 - \exp[\min\{0, -\beta J(\mathbf{S}_i' - \mathbf{S}_i) \cdot \mathbf{S}_j\}]. \quad (3)$$

If the bond between i and j is frozen mark j and add it to the list of sites in the cluster. (e) Continue with step (b) if there are sites on the list which were not visited yet. Otherwise, the growth process stops. Then the cluster is accepted and all its spins are flipped to their new directions \mathbf{S}_i' .

Steps (a) and (d) to (e) reduce to a modified Wolff algorithm. Unlike the original Wolff algorithm, we cannot flip spins as they are joined to the cluster but have to collect them first in a list. This is mandated by the pinning at on-site potentials, which is considered in steps (b) + (c). If the random potentials vanish our extended algorithm produces exactly the same clusters as the Wolff algorithm because clusters are never rejected in (c). Ergodicity of the algorithm (a)–(e) is maintained as in the Wolff algorithm because any spin direction can be flipped into any other by a suitable move, and there is a finite probability of clusters with only one spin. The transition probability W between two configurations $\{\mathbf{S}_i\}$, $\{\mathbf{S}_i'\}$ differing by one flip of a cluster \mathcal{C} factorizes in two parts. The first is due to the change in exchange energy along the boundary of the cluster $\partial\mathcal{C}$, which consists of all bonds with $i \in \mathcal{C}$ and $j \notin \mathcal{C}$. This product of probabilities is identical to the transition probability of the Wolff algorithm in pure models. The second part samples anisotropy energies in the bulk of the cluster. Thus detailed balance is seen by

$$\begin{aligned} \frac{W(\{\mathbf{S}_i\} \rightarrow \{\mathbf{S}_i'\})}{W(\{\mathbf{S}_i'\} \rightarrow \{\mathbf{S}_i\})} &= \prod_{(i,j) \in \partial\mathcal{C}} \frac{1 - P^b(\mathbf{S}_i'; \mathbf{S}_i, \mathbf{S}_j)}{1 - P^b(\mathbf{S}_i; \mathbf{S}_i', \mathbf{S}_j')} \prod_{i \in \mathcal{C}} \frac{P_i^a(\mathbf{S}_i'; \mathbf{S}_i)}{P_i^a(\mathbf{S}_i; \mathbf{S}_i')} \\ &= \exp\left\{ \beta \left[J \sum_{(i,j)} (\mathbf{S}_i' \cdot \mathbf{S}_j' - \mathbf{S}_i \cdot \mathbf{S}_j) \right. \right. \\ &\quad \left. \left. + D \sum_i ((\mathbf{S}_i' \cdot \mathbf{a}_i)^2 - (\mathbf{S}_i \cdot \mathbf{a}_i)^2) \right] \right\}. \quad (4) \end{aligned}$$

Modifying step (c) we get improved algorithms by collecting a number of G on-site terms into one bond to a single ghost spin. This can be built into our algorithm by casting sites together in the sequence in which they are taken from the list during cluster growth. It reads then: (c') Add the on-site energy change ΔE_i^a to a variable ΔE_g^a . When G contributions have been added calculate the probability that this cluster is not pinned at the corresponding group of sites as in

TABLE I. Performance of cluster algorithms for random anisotropy models in $d=2$. Column G gives the respective G value for the cluster algorithm (see text), ‘‘M’’ means Metropolis algorithm. The table lists acceptance ratio a , correlation time τ_M , average cluster sizes $\langle |c| \rangle$ and computation time t_τ per spin to perform τ_M steps (t_τ refer to CPU seconds of a HP-J282).

L	D/J	T/J	G	a	$\langle c \rangle$	τ_M/MCS	t_τ/s
32	0.5	0.95	M	0.296	-	270	1.0e-3
32	0.5	0.95	1	0.305	2.08	6.9	2.1e-4
32	0.5	0.95	4	0.337	3.03	1.5	6.3e-5
32	0.5	0.95	10	0.352	3.92	0.81	4.9e-5
32	0.5	0.95	40	0.368	5.63	0.55	6.4e-5
32	0.5	0.95	100	0.372	6.86	0.53	1.0e-4
32	0.5	0.95	1024	0.375	8.53	0.52	4.7e-4
64	0.5	0.95	M	0.296	-	2360	1.3e-2
64	0.5	0.95	1	0.305	2.08	61	2.1e-3
64	0.5	1.10	10	0.479	6.47	0.96	6.4e-5
16	4.0	1.00	M	0.224	-	516	2.3e-3
16	4.0	1.00	3	0.147	1.15	420	5.3e-3

Eq. (2) but replace the energy ΔE_i^a by this sum of energy changes $\Delta E_g^a \equiv \sum_{i \in \{g\}} \Delta E_i^a$ related to the G sites $\{g\} \subset \mathcal{C}$. If this bond is frozen reject the cluster and start again with (a), otherwise ΔE_g^a is set to zero and the algorithm continues with (d). Detailed balance is still maintained, as seen by a relation similar to Eq. (4) when replacing the product of probabilities $P_i^a(\mathbf{S}_i'; \mathbf{S}_i)$ by products corresponding to groups of sites. Here, we use the number G as a fixed parameter for different algorithms. With G small, the algorithm may miss some correlations and requires more numerical calculations. For large G , much work is spent on useless growth of clusters, which are rejected when pinning is finally considered. In this limit, $G \equiv N$, our algorithm equals the DST algorithm.¹⁹ Thus there is an optimum G .

In the following, we present some simulations for random anisotropy models.²¹ We have sampled equilibrium dynamics starting always with previously well equilibrated spin configurations. Our data indicate that properties do not vary strongly from sample to sample with not too large D/J . As expected, averages calculated with different algorithms for the same sample do not differ. Here, we compare the application of different cluster algorithms and in some cases the Metropolis algorithm. For each method the same set of typically one or two samples of RAM's was used. This is sufficient to determine the performances of the algorithms. They can be measured by the relaxational dynamics seen in the fluctuations of a slow collective mode. We use the magnetization M , which should be the slowest relevant mode and calculate its integrated autocorrelation time τ_M by a self-consistent windowing method.²² Runs for calculating τ_M used at least 10^4 attempted moves per spin (Monte Carlo steps=MCS), but often up to 10^6 MCS. Table I shows results of simulations in $d=2$ dimensions. Note that an accepted move for cluster MC means that on average a number of $\langle |c| \rangle$ spins is flipped, where $\langle |c| \rangle$ is the mean cluster size. The practical efficiency of our algorithm is given by the computation time t_τ to decorrelate a configuration. The data

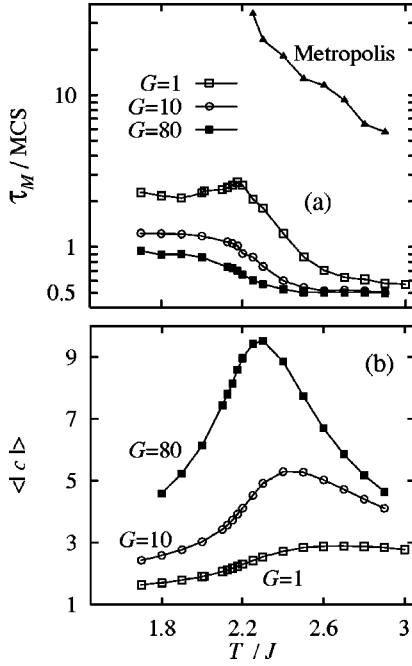


FIG. 1. Temperature dependence of performance data for cluster algorithms with different G values applied to a random anisotropy model ($L=8$, $D/J=1.0$) in $d=3$. (a) Correlation times τ_M —for comparison τ_M for the Metropolis algorithm are included. (b) Average cluster sizes $\langle |c| \rangle$.

show a gain by more than one order of magnitude for the best algorithms for RAM's with $D/J=0.5$ compared to Metropolis MC. There is an optimum performance at a value of $G \approx 10$. For $G > 40$, performance deteriorates leading to rather poor efficiency, as discussed above. The performance data for $D/J=4.0$ show the limitations of our algorithm. The cluster algorithms still reduce τ_M , but practical performance of the algorithms is worse than Metropolis MC. Figure 1 shows the dependence of τ_M and $\langle |c| \rangle$ on temperature in $d=3$ dimensions for a RAM with $D/J=1.0$ and size $L=8$ using different algorithms. Again, a strong reduction of τ_M due to the cluster algorithms as compared to the Metropolis single spin-flip algorithm is found. From Fig. 1(a), it is also seen that with increasing values of G a further reduction of τ_M is achieved, and the divergence of the correlation time can be suppressed. At larger anisotropy strengths $D/J \sim 6$ the cluster algorithm does not produce spanning clusters any more in the critical region and becomes inefficient.

For RAM's in $d=3$ with $D/J=1.0$, an estimate of the critical temperature $T_c/J=2.20$ was obtained previously.⁹ Figure 2 shows scaling of correlation times $\tau_M \propto L^z$ at criticality for cluster algorithms and different values of G . Increasing G reduces always the dynamic exponent z . But at values $G \geq 40$ the performance of the algorithm deteriorates. At optimum values of $G \leq 40$ we have $z \leq 1.0$. For $L=32$, we find that the algorithm with $G=40$ is 20 times faster than the Metropolis algorithm.

We have applied the algorithm with $G=10$ to derive critical properties for RAM's in $d=3$ with $D/J=1.0$ by finite-size scaling. We studied between 25 samples for $L=8, 12$ for $L=48$, and 6 for $L=64$. For each sample, at least of the order 10^4 statistically independent configurations near criticality were simulated for measurements of energy per spin E ,

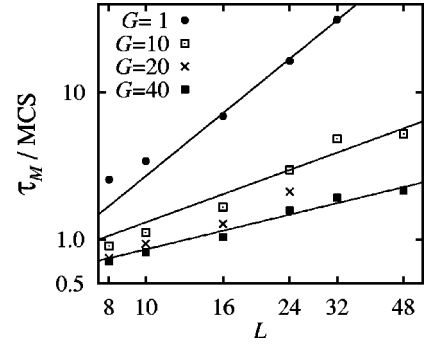


FIG. 2. Correlation time versus system size for random anisotropy models in $d=3$ with $D/J=1.0$ at $T=2.20$. Straight lines $\sim L^z$ with $z=(2.1, 0.9, 0.6)$ are fits to the data for $G=(1, 10, 40)$. (The error of z is about ± 0.2 .)

magnetization M and powers of these quantities. By histogram sampling,²³ we calculate the specific heat $C_L = N([\langle E^2 \rangle]_{av} - [\langle E \rangle]_{av}^2)/T^2$, magnetization $m_L = [\langle M \rangle]_{av}$, connected susceptibility $\chi_L = N([\langle M^2 \rangle]_{av} - [\langle M \rangle]_{av}^2)/T$, disconnected susceptibility $\tilde{\chi}_L = N([\langle M^2 \rangle]_{av})$, and Binder's fourth-order cumulant $U_L = 1 - [\langle M^4 \rangle]_{av} / (3[\langle M^2 \rangle]_{av}^2)$ as functions of T in the critical region. Brackets denote thermal $\langle \dots \rangle$ and sample $[\dots]_{av}$ averages for fixed size L . By calculating these various functions of T separately for individual realizations of the quenched disorder, we find that these functions for the same L do not deviate from each other within about 2σ error bars calculated by the histogram sampling technique. Thus within the accuracy achieved in our runs for individual samples their properties do not differ significantly. The fourth-order cumulant takes on the scaling form $U_L = U[L^{1/\nu}(T - T_c)]$ with ν the correlation length exponent.²⁴ Hence T_c is determined by the unique intersection of the curves $U_L(T)$ for different L , and $1/\nu$ can be determined from a fit $(\partial U_L / \partial T)(T_c) \propto L^{1/\nu}$ as shown in Fig. 3. The relatively small scatter of the intersections for different $U_L(T)$ may be seen as further corroboration that critical properties of different RAM realizations do not differ strongly. With the knowledge of T_c and $1/\nu$, finite-size scaling at T_c yields other critical exponents, using $C_L \propto L^{\alpha/\nu}$, $m_L \propto L^{-\beta/\nu}$, $\chi_L \propto L^{\gamma/\nu}$, and $\tilde{\chi}_L \propto L^{\tilde{\gamma}/\nu}$. We derive the following

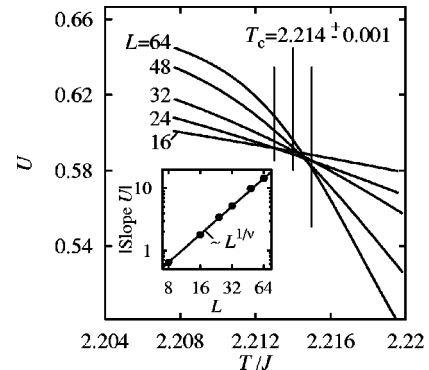


FIG. 3. Fourth-order cumulant U for random anisotropy models in $d=3$ with $D/J=1.0$. From the intersection the critical temperature is determined as indicated by vertical bars. The inset shows the scaling of $(\partial U_L / \partial T)(T_c) \propto L^{1/\nu}$, which yields $1/\nu = 1.498 \pm 0.010$.

values: $T_c/J=2.214\pm 0.001$, $\nu=0.6672\pm 0.005$, $\alpha=0.153\pm 0.003$, $\beta=0.339\pm 0.005$, $\gamma=1.341\pm 0.011$, and $\tilde{\gamma}=1.326\pm 0.011$. Within our accuracy, the scaling relation $2\beta+\tilde{\gamma}=d\nu$ is fulfilled, and the exponents in this relation match those of the XY-ferromagnetic transition.²⁵ But the specific-heat exponent $\alpha>0$ is finite, and the hyperscaling relation $2-\alpha=(d-\theta)\nu$ yields a finite hyperscaling violation exponent $\theta=0.23\pm 0.02$.

In conclusion, we presented a cluster algorithm for disordered magnetic systems. It is very efficient for weak strengths of the on-site potentials in random anisotropy XY models. Critical exponents for these random anisotropy mod-

els in $d=3$ dimensions were determined by a finite-size scaling analysis. The estimated exponents for correlation length, magnetization and susceptibility equal those of the XY-ferromagnetic transition. But our data indicate a different type of transition because we find a divergent specific heat and hyperscaling violation.

I thank L. Schultz for generous support to perform this study, A. Möbius, M. Wolf, and K.-H. Müller for help and useful suggestions, and S. Kobe and his group for discussion. A. Wobst wrote the nucleus of the MC program. This work was supported by INCO-Copernicus.

-
- ¹For recent surveys, see e.g., *Recent Progress in Random Magnets*, edited by D. H. Ryan (World Scientific, Singapore, 1992); *Spin Glasses and Random Fields*, edited by A. P. Young (World Scientific, Singapore, 1998).
- ²D. S. Fisher, M. P. A. Fisher, and D. A. Huse, Phys. Rev. B **43**, 130 (1991); D. A. Huse, Physica B **197**, 540 (1994).
- ³G. Grüner, *Density Waves in Solids* (Addison-Wesley, Reading, MA, 1994).
- ⁴G. G. Batrouni and T. Hwa, Phys. Rev. Lett. **72**, 4133 (1994); H. Rieger, *ibid.* **74**, 4964 (1995); D. Cule and Y. Shapir, *ibid.* **74**, 114 (1995).
- ⁵M. J. P. Gingras and D. A. Huse, Phys. Rev. B **53**, 15 193 (1996); R. Fisch, *ibid.* **57**, 269 (1998).
- ⁶J. M. Kosterlitz and D. J. Thouless, J. Phys. C **6**, 1181 (1973).
- ⁷P. Le Doussal and T. Giamarchi, Phys. Rev. Lett. **74**, 606 (1995).
- ⁸A. J. Bray and M. A. Moore, J. Phys. C **18**, L139 (1985).
- ⁹P. Reed, J. Phys. A **24**, L117 (1991).
- ¹⁰R. Fisch, Phys. Rev. B **39**, 873 (1989); Phys. Rev. Lett. **66**, 2041 (1991); Phys. Rev. B **46**, 242 (1992).
- ¹¹K. Binder *et al.*, in *Applications of the Monte Carlo Method in Statistical Physics*, edited by K. Binder (Springer-Verlag, Berlin, 1987), p. 13, p. 301.
- ¹²R. H. Swendsen and J.-S. Wang, Phys. Rev. Lett. **58**, 86 (1987); J.-S. Wang and R. H. Swendsen, Physica A **167**, 565 (1990), and further references therein.
- ¹³U. Wolff, Phys. Rev. Lett. **62**, 361 (1989).
- ¹⁴R. Gupta and C. F. Baillie, Phys. Rev. B **45**, 2883 (1992); W. Janke and K. Nather, *ibid.* **48**, 7419 (1993); P. Olsson, Phys. Rev. Lett. **73**, 3339 (1994).
- ¹⁵A. Coniglio and W. Klein, J. Phys. A **13**, 2775 (1980).
- ¹⁶R. Harris, M. Plischke, and M. J. Zuckermann, Phys. Rev. Lett. **31**, 160 (1973).
- ¹⁷Y. Imry and S.-K. Ma, Phys. Rev. Lett. **35**, 1399 (1975).
- ¹⁸J.-S. Wang, Physica A **161**, 249 (1989).
- ¹⁹V. S. Dotsenko, W. Selke, and A. L. Talapov, Physica A **170**, 278 (1991).
- ²⁰G. T. Barkema and J. F. Marko, Phys. Rev. Lett. **71**, 2070 (1993).
- ²¹A full description with all details will be given elsewhere.
- ²²U. Wolff, Phys. Lett. B **228**, 379 (1989).
- ²³A. M. Ferrenberg and R. H. Swendsen, Phys. Rev. Lett. **63**, 1195 (1989).
- ²⁴K. Binder, Z. Phys. B **43**, 119 (1981).
- ²⁵J. C. Le Guillou and J. Zinn-Justin, Phys. Rev. B **21**, 3976 (1980).